RSC Advances

RSC Publishing

PAPER

View Article Online
View Journal | View Issue



# Structural variations of D–π–A dyes influence on the photovoltaic performance of dye-sensitized solar cells†

Cite this: *RSC Advances*, 2013, **3**, 7921

Magdalena Marszalek,‡[a] Satyawan Nagane,‡[b] Amol Ichake,[b] Robin Humphry-Baker,[a] Vincent Paul,*[b] Shaik M. Zakeeruddin*[a] and Michael Grätzel*[a]

Received 23rd September 2012,
Accepted 14th March 2013

DOI: 10.1039/c3ra22249g

**www.rsc.org/advances**

Two new organic D–π–A dyes containing identical π-conjugated spacer and anchoring/acceptor moieties but different donor groups were designed and synthesized. These dyes containing didodecyl-cyclopentadithiophene (CPDT) as a spacer, cyanoacrylic acid as an acceptor and *N*-butyl-carbazole or *N*-butyl-phenothiazine moieties as electron donor groups are labelled as **V4** and **V11** dyes, respectively. The variation in the donor group of these two dyes, that influences the photophysical, electrochemical and photovoltaic parameters, was investigated. The highest photovoltaic conversion efficiency of 7.5% was obtained with **V4** dye at AM 1.5 G full sunlight intensity (100 $mWcm^{-2}$). Comparison of phenothiazine donor dyes with two different π-conjugated spacers, CPDT (**V11**) and vinyl thiophene (**V7**) containing devices shows that the $V_{oc}$ of **V7** dye is lower than that of **V11** due to the downward shift of the conduction band edge. Transient photovoltage and electrochemical impedance spectroscopy measurements were performed to explain the differences in the PV parameters by varying the donors and/or spacer groups.

## Introduction

Today, most of the world's energy is produced from fossil fuels. Following rising energy demand and increasingly dire warnings due to the consequences of global warming, solar energy appears to be an excellent alternative to fossil fuel derived energy. Among the technologies that have been developed, dye-sensitized solar cells (DSCs) have aroused great interest in recent years due to low-cost, simple fabrication process and higher conversion efficiency. So far the highest energy conversion efficiency of 12.3% was achieved with DSCs under AM 1.5 G simulated sunlight conditions.[1]

Since the breakthrough of DSCs in 1991, ruthenium polypyridyl complexes have been widely used as efficient sensitizers and a power conversion efficiency of over 11% at full sunlight has been obtained.[2,3] In the past few years there has been growing interest in using metal free organic sensitizers in DSCs and their efficiencies are approaching the values found using ruthenium sensitizers.[4,5] Organic D–π–A dyes have great potential as efficient sensitizers due to their ease of synthesis, the ability to structurally tailor them to tune their photophysical properties, and their higher molar extinction coefficients. An organic D–π–A dye molecule can be divided into three parts; one is the electron rich donor part, another is the anchoring/electron acceptor part, and these two are connected by a π-conjugated spacer. Unfortunately, D–π–A molecules tend to aggregate because of their linear geometry They are much more planar than bulky, spheroidal Ru-complexes. The dye aggregation may already take place in the dye bath solution and also may occur on the $TiO_2$ surface. One of the strategies frequently applied to prevent this phenomenon other than using co-adsorbent molecules is by the introduction of alkyl side chains, which provide steric hindrance and increase intermolecular distances. The electron-rich cyclopentadithiophene unit incorporated into the molecule as a π-bridge, between the donor and acceptor/anchor, strongly enhances light absorption. It is also believed that it influences the surface states of the titania and suppresses charge recombination.[6]

Only a few studies have been reported using carbazole or phenothiazine as donors in D–π–A dyes.[7,8] Recently, Wang *et al.* studied the influence of various aromatic nitrogen donors on the photovoltaic parameters of DSCs, in combination with a cobalt redox electrolyte.[7d] In this paper we investigated the structure–property relation of three dyes (Fig. 1) where two dyes have different donors (*N*-butyl-carbazole, phenothiazine) but the same π-conjugated spacer (CPDT) and the other two dyes contain the same donor

[a]*Laboratory for Photonics and Interfaces, Institute of Chemical Sciences and Engineering, Swiss Federal Institute of Technology, CH-1015 Lausanne, Switzerland. E-mail: shaik.zakeer@epfl.ch; michael.graetzel@epfl.ch; Fax: +41 (0)21 693 61 00; Tel: +41 (0)21 693 31 12*

[b]*Room 288, Organic Chemistry Division, National Chemical Laboratory, Pashan Road, Pune 411008, India. E-mail: vp.swamy@ncl.res.in; Fax: +91 (0)20 2590 2629; Tel: +91 (0)20 2590 2443*

† Electronic supplementary information (ESI) available. See DOI: 10.1039/c3ra22249g

‡ These authors contributed equally to this work.

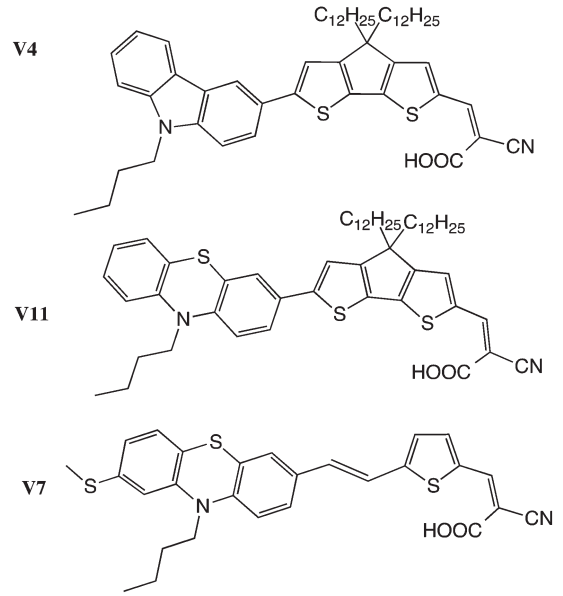


**Fig. 1** Chemical structures of **V4**, **V7** and **V11** dyes.

(phenothiazine) but a different π-conjugated spacer (CPDT and vinyl thiophene).

## Experimental

### Synthesis of 6-(9-butyl-9*H*-carbazol-3-yl)-4,4-didodecyl-4*H*-cyclopenta[1,2-*b*:5,4-*b*′]dithiophene-2-carbaldehyde (3)

In an Ace pressure tube, (9-butyl-9*H*-carbazol-3-yl)boronic acid **1** (0.057 g, 0.21 mmol) and 6-bromo-4,4-didodecyl-4*H*-cyclopenta[1,2-*b*:5,4-*b*′]dithiophene-2-carbaldehyde **2** (0.11 g, 0.177 mmol) were dissolved in THF, followed by addition of aqueous $K_2CO_3$ (2 M, 1 mL). The reaction mixture was degassed with argon for 30 min, $Pd(PPh_3)_4$ (0.02 g, 0.017 mmol) was added under an inert atmosphere, and the reaction mixture was degassed again for 15 min. The entire reaction mixture was heated at 80 °C for 7 h. After completion of the reaction (monitored by TLC), the reaction mixture was diluted with ethyl acetate and the organic layer washed with water. The organic layer was dried over sodium sulfate and concentrated under reduced pressure to afford the crude product, which was purified using column chromatography (eluent: ethyl acetate–petroleum ether, 5 : 95) to afford **3** (0.120 g, 89% yield). $^1$H NMR (400 MHz, chloroform-*d*): δ (ppm): 0.86 (t, 6H, $CH_3$), 0.95 (t, 5H, $CH_2$, $CH_3$), 1.14–1.27 (m, 38H, $CH_2$), 1.46 (m, 2H, $CH_2$), 1.77–1.89 (m, 6H, $CH_2$), 3.87 (t, 2H, $CH_2$), 6.85 (d, 1H, ar), 6.88 (d, 1H, ar), 6.93 (t, 1H, ar), 7.09 (s, 1H, ar), 7.13–7.18 (m, 2H, ar), 7.38 (m, 2H, ar), 7.55 (s, 1H, ar), 9.81 (s, 1H, CHO). $^{13}$C NMR (100 MHz, chloroform-*d*): δ (ppm): 13.86, 14.09, 20.52, 22.64, 24.61, 29.31, 29.36, 29.59, 29.98, 31.10, 31.86, 37.73, 42.97, 54.07, 109.01, 109.15, 116.59, 117.55, 119.22, 120.53, 122.64, 123.36, 123.87, 125.56, 126.15, 130.03, 133.37, 140.32, 140.94, 142.51, 148.55, 151.27, 157.11, 163.77, 182.37. HRMS-ESI (*m*/*z*) $[M]^+$ calculated for $C_{50}H_{69}NOS_2$, 763.4821; found, 763.9366 (1%): $[M+H]^+$ calculated for $C_{50}H_{70}NOS_2$, 764.4899; found, 764.4946 (100%).

### Synthesis of (*E*)-3-(6-(9-butyl-9*H*-carbazol-3-yl)-4,4-didodecyl-4*H*-cyclopenta[1,2- *b*:5,4-*b*′]dithiophen-2-yl)-2-cyanoacrylic acid (V4)

To a solution of 6-(9-butyl-9*H*-carbazol-3-yl)-4,4-didodecyl-4*H*-cyclopenta[1,2-*b*:5,4-*b*′]dithiophene-2-carbaldehyde **3** (0.12 g, 0.16 mmol) in dry toluene, cyanoaceticacid (0.020 g, 0.23 mmol) was added under an inert atmosphere. To the stirring reaction mixture, piperidine (0.020 g, 0.23 mmol) was added dropwise. The entire reaction mixture was refluxed for 7 h. After completion of the reaction (monitored by TLC), the solvent was distilled out under reduced pressure, to afford the crude product, which was purified by column chromatography (eluent: methanol–dichloromethane, 5 : 95) on silica gel to afford **V4** as a red solid (0.105 g, 81% yield). $^1$H NMR (500 MHz, chloroform-*d*): δ (ppm): 0.84 (t, 6H, $CH_3$), 0.95 (t, 3H, $CH_3$), 1.21 (m, 40H, $CH_2$), 1.38 (m, 2H, $CH_2$), 1.85 (m, 2H, $CH_2$), 1.95 (m, 4H, $CH_2$), 4.29 (t, 2H, $CH_2$), 7.25–7.28 (m, 2H, ar), 7.38–7.44 (m, 2H, ar), 7.50 (t, 1H, ar), 7.64 (s, 1H, ar), 7.73 (d, 1H, ar), 8.13 (d, 1H, ar), 8.32 (d, 2H, ar). $^{13}$C NMR (125 MHz, chloroform-*d*): δ (ppm): 13.86, 14.09, 20.52, 22.66, 24.64, 29.31, 29.37, 29.58, 29.61, 29.62, 29.95, 31.10, 31.88, 37.80, 42.96, 54.20, 91.46, 109.05, 109.20, 116.60, 117.11, 117.66, 119.33, 120.60, 122.65, 123.40, 123.93, 125.29, 126.23, 133.45, 135.56, 140.53, 140.95, 148.03, 152.09, 153.49, 158.14, 165.27, 169.27. HRMS-ESI-TOF-MS(ES-) (*m*/*z*) $[M]^+$ calculated for $C_{53}H_{70}N_2O_2S_2$, 830.4879; found, 830.4833 (60%): $[M-H]^+$ calculated for $C_{53}H_{69}N_2O_2S_2$, 829.4800; found, 829.4800 (100%).

### Synthesis of 6-(10-butyl-10*H*-phenothiazin-3-yl)-4,4-didodecyl-4*H*-cyclopenta[1,2-*b*:5,4-*b*′]dithiophene-2-carbaldehyde (5)

In an Ace pressure tube, (10-butyl-10*H*-phenothiazin-3-yl)boronic acid **4** (0.115 g, 0.39 mmol) and 6-bromo-4,4-didodecyl-4*H*-cyclopenta[1,2-b:5,4-b′]dithiophene-2-carbaldehyde **2** (0.2 g, 0.32 mmol) were dissolved in THF followed by addition of aqueous $K_2CO_3$ (2 M, 1.5 mL). The reaction mixture was degassed with argon for 30 min. $Pd(PPh_3)_4$ (0.037 g, 0.032 mmol) was added under an inert atmosphere and the reaction mixture was degassed again for 15 min. The entire reaction mixture was then heated at 70–80 °C for 9–10 h. After completion of the reaction (monitored using TLC), the reaction mixture was diluted with ethyl acetate and the organic layer washed with water. The organic layer was dried over sodium sulfate and concentrate under reduced pressure to afford the crude product, which was purified using column chromatography (eluent: ethyl acetate–petroleum ether, 5 : 95) to afford **5** (0.220 g, 86% yield). $^1$H NMR (400 MHz, chloroform-*d*): δ (ppm): 0.86 (t, 6H, $2CH_3$), 0.95 (m, 7H, $2CH_2$, $CH_3$), 1.14–1.29 (m, 36H, $CH_2$), 1.46 (m, 2H, $CH_2$), 1.76–1.93 (m, 6H, $CH_2$), 3.85 (t, 2H, $CH_2$), 6.82–6.84 (d, 1H, $J$ = 9.03 Hz, ar), 6.85–6.87 (d, 1H, $J$ = 8.03 Hz, ar), 6.92 (t, 1H, $J$ = 7.78, 7.28 Hz, ar), 7.10 (s, 1H, ar) 7.11–7.17 (m, 2H, ar), 7.37 (m, 2H, ar), 7.55 (s, 1H, ar), 9.81 (s, 1H, CHO). $^{13}$C NMR(100 MHz, chloroform-*d*): δ (ppm): 13.75, 14.08, 20.07, 22.62, 24.55, 28.83, 29.27, 29.31, 29.53, 29.56, 29.91, 31.84, 37.59, 47.14, 53.99, 115.37, 115.43, 116.72, 122.55, 123.87, 124.09, 124.54, 125.51, 127.32, 127.38,

 

128.73, 129.90, 133.81, 142.83, 144.61, 144.94, 148.00, 148.55, 157.34, 163.42, 182.31. HRMS-ESI (*m*/*z*) $[M]^+$ calculated for $C_{50}H_{69}NOS_3$, 795.4541; found, 795.4540 (30%): $[M+H]^+$ calculated for $C_{50}H_{70}NOS_3$, 796.4620; found, 796.4622 (100%).

### Synthesis of (*E*)-3-(6-(10-butyl-10*H*-phenothiazin-3-yl)-4,4-didodecyl-4*H*-cyclopenta[1,2-*b*:5,4-*b*′]dithiophen-2-yl)-2-cyanoacrylic acid (V11)

To a solution of 6-(10-butyl-10*H*-phenothiazin-3-yl)-4,4-didodecyl-4*H*-cyclopenta[1,2-*b*:5,4-*b*′]dithiophene-2-carbaldehyde **5** (0.203 g, 0.3 mmol) in dry toluene, cyanoaceticacid (0.042 g, 0.5 mmol) was added under an inert atmosphere. To the stirring reaction mixture, piperidine (0.042 g, 0.5 mmol) was added dropwise. The entire reaction mixture was refluxed for 7 h. After completion of the reaction (monitored using TLC), the solvent was distilled out under reduced pressure and the crude product was purified using silica gel column chromatography (eluent: methanol–dichloromethane, 5 : 95) to afford **V11** as a red solid (0.105 g, 81% yield). $^1$H NMR (400 MHz, chloroform-*d*): $\delta$ (ppm): 0.84 (t, 6H, $CH_3$), 0.92 (t, 3H, $CH_3$), 1.03 (bs, 4H, $CH_2$), 1.16–1.25 (m, 36H, $CH_2$), 1.41 (m, 2H, $CH_2$), 1.72 (m, 2H, $CH_2$), 1.88 (bs, 4H, $CH_2$) 3.71 (bs, 2H, $CH_2$), 6.63 (d, 1H, $J$ = 7.53 Hz, ar), 6.79 (d, 1H, $J$ = 8.03 Hz, ar), 6.91 (t, 1H, $J$ = 7.53 Hz, ar), 7.09–7.16 (m, 3H, ar), 7.22 (s, 2H, ar), 7.63 (s, 1H, ar), 8.37 (s, 1H, ar). $^{13}$C NMR (100 MHz, chloroform-*d*): $\delta$ (ppm): 13.63, 13.94, 19.98, 22.53, 24.44, 28.78, 29.20,29.47, 29.78, 31.76, 37.59, 47.13, 54.04, 93.85, 115.38, 115.41, 116.72, 117.60, 122.57, 123.78, 124.08, 124.62, 125.49, 127.32, 128.27, 128.57, 130.68, 133.86, 135.86, 144.55, 145.12, 147.04, 149.53, 158.02. 164.02, 165.59. HRMS-ESI-TOF-MS (ES+) (*m*/*z*) $[M]^+$ calculated for $C_{53}H_{70}N_2O_2S_3$, 862.4599; found, 862.4661.

### Characterization of the sensitizers

All chemicals were purchased from commercial sources (Sigma-Aldrich, Merck and TCI) and used without further purification. Solvents used as reaction media were purchased from local sources and used after distillation. Petroleum ether (PE) refers to the fraction boiling in the range of 40–60 °C. Reactions were monitored using analytical TLC plates (Merck, silica gel 60 F254, 0.25 mm) and compounds were resolved with ultraviolet light. Silica gel (100–200 and 230–400 mesh) was used for column chromatography. $^1$H and $^{13}$C NMR spectra were recorded on a Bruker-AV 200, 400, 500 spectrometer, in chloroform-*d* (Sigma-Aldrich) using TMS as an internal standard. The chemical shift values are reported in ppm ($\delta$) units and the coupling constants ($J$) in Hz. All synthesized compound structures were confirmed using $^1$H and $^{13}$C NMR. HRMS spectra were obtained on a Thermo Scientific Q-Exacative, Accela 1250 pump. The absorption spectra of **V4** and **V11** were measured in dichloromethane with a CARY 5 UV-Vis-NIR spectrophotometer (Varian, Inc.). Steady-state excited state emission spectra were measured on a FluoroLog-322 (Horiba) spectrometer equipped with a 450 W Xe arc lamp using dilute dye solutions ($10^{-6}$ M) in dichloromethane solvent.

### Differential pulse voltammetry (DPV) measurements

The DPV of the dyes was measured with an Autolab PGSTAT30 potentiostat. The measurements were carried out in dichloromethane (Acros Organics) solution containing tetrabutylammonium hexafluorophosphate (0.1 M) (Fluka) as a supporting electrolyte with glassy carbon as the working electrode and Pt as the counter electrode under an Ar atmosphere. The redox potentials were calibrated with ferrocene as the internal reference.

### Cell fabrication

Dye sensitized solar cells were fabricated using a double-layered photoanode made of mesoporous $TiO_2$. A transparent, 8-μm-thick layer of 20 nm particles was screen-printed onto a FTO glass pane (NSG-10, Nippon Sheet Glass), pre-treated with $TiCl_4$. Subsequently, a 5-μm-thick layer of scattering particles (400 nm diameter) was screen-printed and the thus formed electrode was sintered up to 500 °C. $TiCl_4$ post-treatment was performed onto the substrates in order to increase the surface area. The photoanodes were sintered again and after cooling down to 80 °C immersed in the dye solutions for 16 h. The solutions contained 0.1 mM of the **V4** or **V11** dye in dichloromethane. After rinsing with the same solvent, the stained substrates were sealed with pieces of thermally platinized (a drop of 8 mM hexachloroplatinic acid solution in 2-propanol, heated to 425 °C) FTO glass (TEC15, Pilkington), which served as a counter electrode. 25-μm-thick Surlyn (Dupont) was used as a binder and a spacer. The electrolytes were introduced to the cells *via* pre-drilled holes in the counter electrodes. The composition of the electrolyte was as follows: 1.0 M 1,3-dimethylimidazolium iodide, 0.03 M iodine, 0.1 M guanidinium thiocyanate, 0.5 M *tert*-butylpyridine, 0.05 M lithium iodide in acetonitrile–valeronitrile (85 : 15, v/v). The DSC devices were measured 24 h after fabrication.

### Photovoltaic characterization

The setup used for standard photovoltaic characterization ($J$–$V$ curve) consisted of a 450 W xenon lamp (Oriel), whose spectral output was matched in the region of 350–750 nm with the aid of a Schott K113 Tempax sunlight filter (Präzisions Glas & Optik GmbH), and a source meter (Keithley 2400) to apply potential bias and measure the photogenerated current. A set of metal mesh filters was used to adjust the light intensity to a desired level. IPCE was measured using a SR830 lockin amplifier, however the incident light (300 W xenon lamp, ILC Technology) was focused through a Gemini-180 double monochromator (Jobin-Yvon Ltd.). The cells were measured with an external light bias (100 W $m^{-2}$ intensity) provided by an LED array. A black metal mask defined the cell active area to be 0.159 $cm^2$.

### Transient photovoltage and photocurrent experiment

Both transient decays were measured under varying white light bias provided by a LED array with superimposed red perturbation pulses (also LED). A source meter (Keithley 2602) was employed to record the voltage dynamics. Photovoltage decays were measured at different open-circuit potentials defined by varying the white light intensity. Cell capacitance was obtained from the integrated photocurrent decay measured close to $V_{oc}$ (varying the light intensity as well). Red perturbation pulses were controlled not to exceed

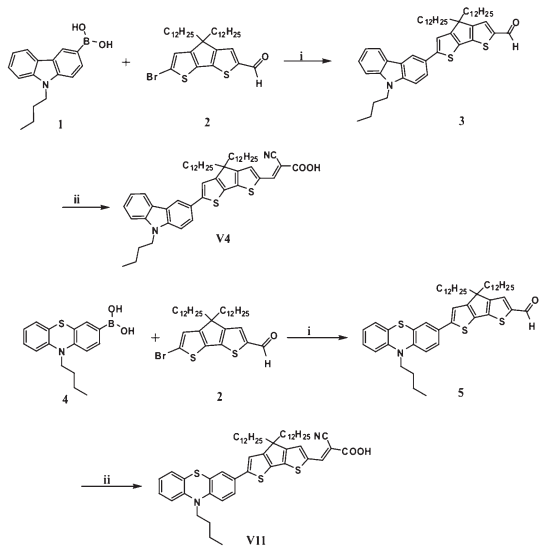

**Scheme 1** (i) $Pd(PPh_3)_4$, $K_2CO_3$, THF, $H_2O$, 80 °C, 7 h. (ii) Cyanoaceticacid, piperidine, toluene, reflux, 7 h.

5% of the signal resulting from the white bias (either current or voltage) in order to maintain single-exponential decay.[9]

### Electrochemical impedance spectroscopy (EIS)

The EIS analysis was done on DSC devices at a constant temperature of 20 °C in the dark. A sinusoidal potential perturbation of an amplitude of 10 mV was applied over a frequency range 1 MHz–0.1 Hz (Autolab PGSTAT30 potentiostat) for a constant potential bias varied between 300 mV and 750 mV with a 25 mV step. The spectra were fitted using ZView software (Scribner Associates) using the transmission line model.[10] The potential was corrected for the ohmic losses on the series resistance of the cell.

## Results and discussion

### Synthetic route

The sensitizers **V4** and **V11** were synthesized as depicted in Scheme 1. Compounds **1**, **2** and **4** were synthesized *via* reported methods.[11] The Suzuki coupling of aldehyde **2** with (9-butyl-9*H*-carbazol-3-yl)boronic acid **1** afforded compound **3** in 89% yield after column chromatography. Knoevenagel condensation of this aldehyde **3** with cyanoacetic acid afforded the desired sensitizer **V4** as a red solid in 81% yield. Similarly, intermediate **5** was synthesized by Suzuki coupling of aldehyde **2** with (10-butyl-10*H*-phenothiazin-3-yl)boronic acid **4**, which on Knoevenagel condensation with cyanoacetic acid afforded sensitizer **V11** as a red solid in 81% yield.

The UV-vis absorption spectra recorded for the **V4** and **V11** dyes in dichloromethane are shown in Fig. 2. The lowest energy peak position and molar absorption coefficients are tabulated in Table 1. The lowest energy absorption band for the **V4** and **V11** dyes is located at 532 nm, corresponding to intramolecular charge transfer from the *N*-butyl-carbazole or

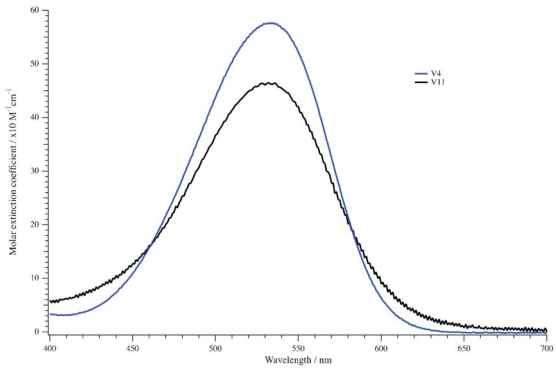


**Fig. 2** UV-Vis spectra of the **V4** (blue) and **V11** (black) dyes in dichloromethane.

the *N*-butyl-phenothiazine donor to the cyanoacrylic acid, providing efficient charge separation at the excited state. **V4** dye with *N*-butyl-carbazole donor has the highest molar extinction coefficient, reaching up to 57 500 $M^{-1}$ $cm^{-1}$. When *N*-butyl-carbazole is compared to *N*-butyl-phenothiazine as a donor group, a stronger influence on the molar extinction coefficient of the dye is witnessed on the low energy absorption peak position. The photoluminescence maximum of **V4** and **V11** dyes in dichloromethane solvent is observed at 636 nm and 610 nm, respectively. Emission measurements in combination with UV-vis spectra do not exhibit significant differences in the Stokes shift between the dyes.

It is important to determine the highest occupied molecular orbital (HOMO) and lowest unoccupied molecular orbital (LUMO) energy of the dye molecules in order to know whether there is enough driving force to inject electrons into the $TiO_2$ conduction band and to afford the regeneration of the dye cation with the redox electrolyte. The electrochemical properties of the dyes were studied with differential pulse voltammetry to obtain formal redox potentials of the molecules and are presented in the Table 1. The oxidation potential of **V11** dye is observed at 1.15 V, which is in agreement with the reported values of **V7** which has *N*-butyl-(2-methylthio)-phenothiazine as a donor. The oxidation potential of **V4** dye is 180 mV more positive than that of **V7** dye, indicating that the HOMO is stabilized more in the presence of the *N*-butyl-carbazole donor than the *N*-butyl-(2-methylthio)-phenothiazine donor moiety. The excited state reduction potentials of **V4**

**Table 1** Absorption, emission and electrochemical properties of **V4** and **V11** dyes measured in dichloromethane

| Dye | **V4** | **V11** |
|---|---|---|
| $\lambda_{(\varepsilon)}$ /nm ($M^{-1}$ $cm^{-1}$) | 532 (57 500) | 532 (46 500) |
| $\lambda$ (emission) /nm | 636 | 610 |
| Ox /V[a] | 1.15 | 0.97 |
| $E_{0-0}$ /eV[b] | 2.11 | 2.20 |
| ($E_{ox}$ − $E_{0-0}$) /V | −0.96 | −1.23 |

[a] Oxidation potentials measured with ferrocene as an internal standard and the values are given *vs.* NHE. (Ferrocene = +0.7 *vs.* NHE). [b] $E_{0-0}$ transition energy was estimated from the emission and absorption spectra.

 

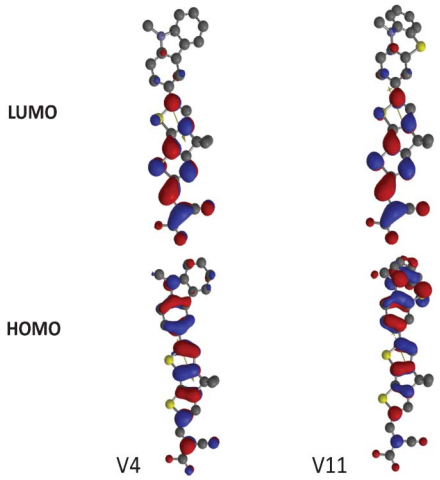


**Fig. 3** Frontier molecular orbitals calculated for the simplified **V4** and **V11** dyes in vacuum.

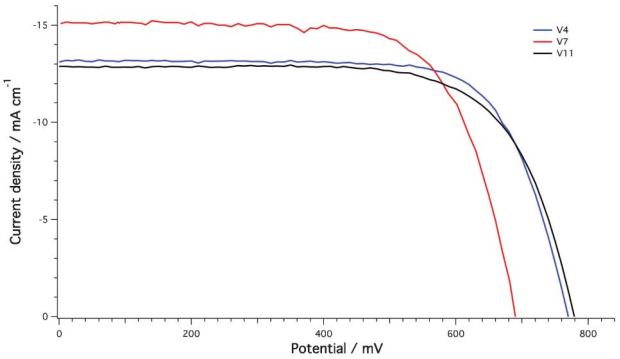


**Fig. 4** Photocurrent density as a function of applied voltage recorded under 1 sun illumination for devices with V-dyes and a volatile electrolyte.

and **V11** dyes were obtained by combining the oxidation potentials with the energy of the transition upon light absorption. The excited state potentials are placed sufficiently above the $TiO_2$ conduction band edge (−0.5 V *vs.* NHE) to ensure no energetic barriers for the electron injection. Since the HOMO energy levels of the **V4** and **V11** dyes are both above 0.90 V *vs.* NHE, higher than the redox energy level of the $I^-/I_3^-$ couple (0.35 V *vs.* NHE), there should be enough driving force for dye regeneration.

In order to get more insight into the molecular structure and electron distribution within the molecules, DFT calculations were performed. These analyses were carried out using B3LYP/6-31G basis set to optimize dye geometries and energies. The molecules were simplified by replacing alkyl chains attached to the CPDT, carbazole and phenothiazine units with methyl groups to reduce the number of basis functions. Initial optimization of the geometry of the molecules reveals that the carbazole donor is the least distorted from planarity. The phenothiazine donor exhibits a fold along the sulphur–nitrogen axis going through the middle ring. As can be seen in Fig. 3, the HOMO orbitals are mainly located at the donor end of the molecule. There is some extension of the HOMO onto the π-conjugated building block. Nevertheless, the LUMO is confined to the π-bridge and acceptor in all cases, which confirms that there should be no problem with effective charge separation and subsequent injection of an electron into the titania conduction band.

DSCs were fabricated as explained in the experimental section, using a double-layer-$TiO_2$ nanostructured film (8 μm transparent layer coated with 5 μm scattering layer) and a standard Pt counter electrode. All the DSCs were characterized under standard AM 1.5 G irradiation. The *J–V* curves of the devices are shown in Fig. 4 and the photovoltaic parameters are presented in Table 2.

The incident photon-to-conversion efficiency (IPCE) of devices sensitized with **V4** and **V11** exhibit a plateau of 70 to 80% from 450 nm to 600 nm as shown in Fig. 5. The **V11** dye sensitized device exhibits somewhat lower IPCE values compared to the **V4** dye. A maximum IPCE of 86% at 600 nm was obtained with the **V4** dye (Fig. 5), which is in agreement with the proposed optical and internal loss mechanisms for a DSC. In the absence of antireflection UV cut-off film on top of the devices, the reflections from the glass surface account for 10% of the losses. Since IPCE is a product of the efficiencies of three consecutive processes occurring within the cell: light harvesting, electron injection and charge collection, it could then be inferred that none of the above listed phenomena impedes the work of the devices, and they are close to their peak performance.

The IPCE spectral response for **V4** and **V11** dyes reaches up to 700 nm whereas for the **V7** device it extends up to 750 nm (Fig. 5). The higher $J_{sc}$ values obtained with the **V7** dye are due to the broader spectral response in the IPCE spectrum of **V7** dye. The differences in the IPCE spectra of **V7** dye compared to **V4** and **V11** are in agreement with the red shift in the absorption spectra adsorbed on a transparent $TiO_2$ film, respectively (as shown in Fig. S2, ESI†). In addition to the red shifted spectral response, the concentration of **V7** dye adsorbed on the $TiO_2$ film is higher than that of the **V4** and **V11** dyes due to its smaller molecular size (Table S1, ESI,†), which contributes to the higher $J_{sc}$ value that was observed in the *J–V* measurements.

Devices with **V4** and **V11** dyes yielded power conversion efficiencies (PCE) of 7.5 and 7.0% respectively at full sunlight intensity under standard AM 1.5 G conditions. Both these devices show comparable PCE with similar $J_{sc}$ and $V_{oc}$ values as shown in Table 2. This shows that there is not much influence of the donor group on the devices' PCE values, whether it is *N*-butyl-carbazole or *N*-butyl-phenothiazine. Here we would like to make comparisons with a similar D–π–A dye **V7**,[4f] which

**Table 2** Summarized photovoltaic parameters of DCSs sensitized with the **V**dyes

| Dye | **V7** | **V11** | **V4** |
|---|---|---|---|
| $J_{sc}$ /mA cm$^{-2}$ | 15.2 | 12.9 | 13.1 |
| $V_{oc}$ /mV | 691 | 774 | 770 |
| Fill factor | 0.70 | 0.70 | 0.73 |
| $\eta$ /% | 7.4 | 7.0 | 7.5 |

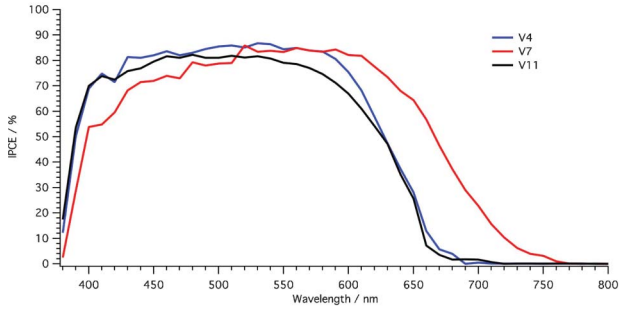


**Fig. 5** Incident photon-to-current efficiency spectra for the champion devices sensitized with V-dyes.

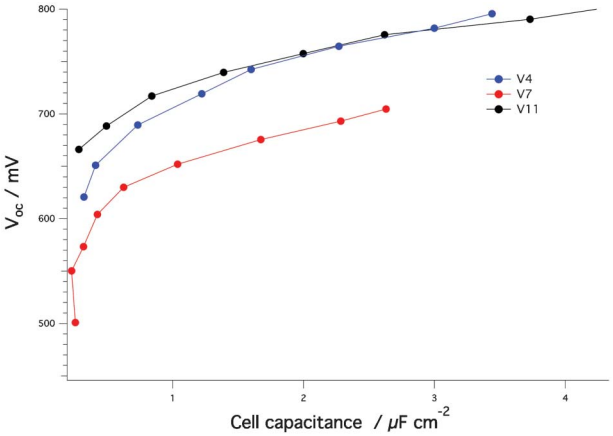


**Fig. 6** Representation of the densities of states for three devices given by the $V_{oc}$ *vs.* cell capacitance obtained through transient measurements.

has *N*-butyl-(2-methylthio)-phenothiazine as a donor and its π-conjugated spacer is vinyl thiophene, replacing the CPDT of **V11** dye. Maintaining identical $TiO_2$ films, redox electrolyte and counter electrodes, the only difference in the devices is the structure of two dyes, which have different π-conjugated spacers. This comparison gives us more insight into the structure–performance relationship of D–π–A dyes within the context of photovoltaic performance. The photovoltaic parameters of **V7** devices compared to **V11** dye-sensitized devices show larger differences in the $J_{sc}$ and $V_{oc}$ values. The $J_{sc}$ and $V_{oc}$ values of **V7** and **V11** devices are 15.2 mA cm$^{-2}$, 691 mV and 12.9 mA cm$^{-2}$, 774 mV, respectively.

To better understand the difference in the $V_{oc}$ of **V7** and **V4**/**V11** devices, transient photovoltage decay characterization was done on both devices and compared to the reported values of the **V7** device. The **V7** cell, with the 80 mV lower $V_{oc}$ than **V4**/**V11**, exhibited the highest current density. The trapped electron density estimated from the short-circuit current density in the cell with **V7** is higher than for **V4**/**V11**. Under short-circuit conditions, the recombination flux is negligible thus $J_{sc}$ is a good measure of the electrons in the film.[12] Taking the ratio of the number of charges approximated from the corresponding short-circuit current densities (Table 2) we find that the calculated change in $V_{oc}$ between **V4**/**V11** and **V7** is about 10 mV. This suggests that a 70 mV difference is arising due to a shift in the conduction band position.

For all three devices the $V_{oc}$ measured under decreasing light intensity against cell capacitance is plotted in Fig. 6. Cell capacitance is related to the density of states in the semiconductor *via* the following equation:

$$DOS = \frac{C_\mu}{d(1-p)e} \quad (1)$$

where $d$ is the thickness of the active $TiO_2$ layer, $p$ is the porosity and $e$ is the elementary charge. The **V7** sensitized cell shows the lowest lying quasi-Fermi level as compared to the other devices, which is in line with the $V_{oc}$ as measured during standard *J*–*V* characterization. As a consequence of the higher surface concentration of **V7** dye, an increased concentration of protons on the surface of $TiO_2$ film might be expected. This would be responsible for shifting the DOS of the **V7** device.

The DSCs were further subjected to electrochemical impedance spectroscopy (EIS) investigation. The derived electron transfer resistance at the dye-sensitized $TiO_2$–electrolyte interface was obtained by fitting the EIS data in Fig. S3, ESI.† The electron transfer resistance is related to the electron concentration inside the $TiO_2$ and that of the concentration of oxidized species of the redox couple.[13] Considering the conduction band edge difference, a 70 mV offset of Rct for **V7** along the applied voltage axis (see Fig. 7) indicates that the interfacial recombination of these devices is similar under an identical potential. This is also supported by the apparent electron lifetime plot (Fig. S4, ESI†), where the traces for the respective dyes lie relatively close to each other, especially at the high capacitance conditions. Under these conditions, the variation of the recombination rates is minor in terms of cell capacitance, which represents an indirect measure of the Fermi level. This confirms that the observed differences in $V_{oc}$ for these devices with **V4**, **V7** and **V11** dyes are mainly due to the shift in the conduction band.

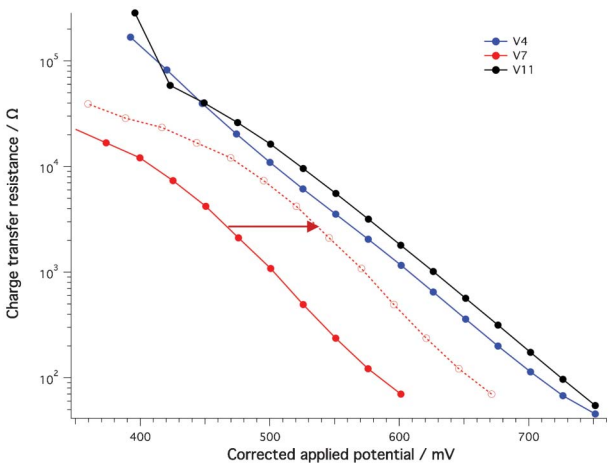


**Fig. 7** Charge transfer resistance derived from electrochemical impedance spectroscopy against applied voltage corrected for the IR drop. The arrow indicates a 70 mV positive shift derived from the transient measurements; the shifted resistance values of **V7** lie close to the values of the **V4**/**V11** dyes.

When comparing the two dyes with CPDT as a spacer (**V4** and **V11**), the electronic properties of the interface remained unchanged; the devices sensitized with **V4** and **V11** dyes exhibit similar capacitances and charge transfer resistances. One can conclude that the donor part of the dye is not affecting the nature of the interface and device performance. The molecules' structural units like alkyl chains substituted on the chromophore of the CPDT have more impact on the dye loading and conduction band edge position.

## Conclusions

In this work we presented a photovoltaic data comparison between three D–π–A dyes, two of them sharing identical π-conjugated bridge and anchoring groups and differing only in their donor groups, namely *N*-butyl-phenothiazine and *N*-butyl-carbazole. Another set of two dyes containing the same donor and anchoring group, differing only in their π-conjugated spacer, namely didodecyl CPDT and vinyl thiophene are also compared. These results show that two different donors have an insignificant influence on the device performance, but substituting a bulky CPDT unit in place of a vinyl thiophene as a π-bridge, has remarkable influence on the device $V_{oc}$ due to a shift in the conduction band edge. This particular choice of dyes for comparison allows for a direct insight into the interface between the sensitized film and electrolyte in the design of new dye molecules, which paves the way for the enhancement of the DSC device performance.

## Acknowledgements

MG thanks the Swiss National Science Foundation for financial support under the Indo-Swiss Joint Research Programme (ISJRP) grant. VP wishes to acknowledge financial support from the Department of Science & Technology, New Delhi, sponsored under the Indo-Swiss Joint Research Project (INT/ SWISS/*P*-33/2009). We are grateful to Nippon Sheet Glass Co., Ltd, and Mihama Co., for providing the FTO glass and the antireflection layer, respectively. We also thank Mr Pascal Comte for providing us with the $TiO_2$ films used in this study and Dr Carole Grätzel for fruitful discussions.

## References

1 A. Yella, H.-W. Lee, H. N. Tsao, C. Yi, A. K. Chandiran, M. K. Nazeeruddin, E. W.-G. Diau, C.-Y. Yeh, S. M. Zakeeruddin and M. Grätzel, *Science*, 2011, **334**, 629.

2 M. Grätzel, *Acc. Chem. Res.*, 2009, **42**, 1788.

3 (*a*) C. Chen, M. Wang, J. Li, N. Pootrakulchote, L. Alibabaei, C. Ngoc-le, J. Decoppet, J. Tsai, C. Grätzel, C. Wu, S. M. Zakeeruddin and M. Grätzel, *ACS Nano*, 2009, **3**, 3103; (*b*) F. Gao, Y. Wang, D. Shi, J. Zhang, M. Wang, X. Jing, R. Humphry-Baker, P. Wang, S. M. Zakeeruddin and M. Grätzel, *J. Am. Chem. Soc.*, 2008, **130**, 10720; (*c*) Q. Yu, Y. Wang, Z. Yi, N. Zu, J. Zhang, M. Zhang and P. Wang, *ACS Nano*, 2010, **4**, 6032; (*d*) Y. Chiba, A. Islam, Y. Watanabe, R. Komiya, N. Koide and L. Han, *Jpn. J. Appl. Phys.*, 2006, **45**, L638.

4 (*a*) G. Zhang, H. Bala, Y. Cheng, D. Shi, X. Lv, Q. Yu and P. Wang, *Chem. Commun.*, 2009, 2198; (*b*) W. Zeng, Y. Cao, Y. Bai, Y. Wang, Y. Shi, M. Zhang, F. Wang, C. Pan and P. Wang, *Chem. Mater.*, 2010, **22**, 1915; (*c*) S. Ito, H. Miura, S. Uchida, M. Takata, K. Sumioka, P. Liska, P. Comte, P. Péchy and M. Grätzel, *Chem. Commun.*, 2008, 5194; (*d*) R. Li, J. Liu, N. Cai, M. Zhang and P. Wang, *J. Phys. Chem. B*, 2010, **114**, 4461; (*e*) W. Zhu, Y. Wu, S. Wang, W. Li, X. Li, J. Chen, Z. S. Wang and H. Tian, *Adv. Funct. Mater.*, 2011, **21**, 756; (*f*) M. Marszalek, S. Nagane, A. Ichake, R. Humphry-Baker, V. Paul, S. M. Zakeeruddin and M. Grätzel, *J. Mater. Chem.*, 2012, **22**, 889; (*g*) C. Qin, A. Islam and L. Han, *Dyes Pigm.*, 2012, **94**, 553.

5 (*a*) A. Mishra, M. Fischer and P. Bäuerle, *Angew. Chem., Int. Ed.*, 2009, **48**, 2474 and references cited therein; (*b*) L. Alibabaei, J.-H. Kim, M. Wang, N. Pootrakulchote, J. Teuscher, D. Di Censo, R. Humphry-Baker, J.-E. Moser, Y.-J. Yu, K.-Y. Kay, S. M. Zakeeruddin and M. Grätzel, *Energy Environ. Sci.*, 2010, **3**, 956; (*c*) A. Hagfeldt, G. Boschloo, L. Sun, L. Kloo and H. Pettersson, *Chem. Rev.*, 2010, **110**, 6595 and references cited therein.

6 R. Li, J. Liu, N. Cai, M. Zhang and P. Wang, *J. Phys. Chem. B*, 2010, **114**, 4461.

7 (*a*) D. Kim, J. K. Lee, S. O. Kang and J. Ko, *Tetrahedron*, 2007, **63**, 1913; (*b*) Z. Wan, C. Jia, L. Zhou, W. Huo, X. Yao and Y. Shi, *Dyes Pigm.*, 2012, **95**, 41; (*c*) C. Teng, X. Yang, C. Yuan, C. Li, R. Chen, H. Tian, S. Li, A. Hagfeldt and L. Sun, *Org. Lett.*, 2009, **11**, 5542; (*d*) M. Xu, D. Zhou, N. Cai, J. Liu, R. Li and P. Wang, *Energy Environ. Sci.*, 2011, **4**, 4735.

8 (*a*) M. H. Tsao, T. Y. Wu, H. P. Wang, I. W. Sun, S. G. Su, Y. C. Lin and C. W. Chang, *Mater. Lett.*, 2011, **65**, 583; (*b*) D. Cao, J. Peng, Y. Hong, X. Fang, L. Wang and H. Meier, *Org. Lett.*, 2011, **13**, 1610.

9 (*a*) B. C. O'Regan and F. Lenzmann, *J. Phys. Chem. B*, 2004, **108**, 4342–4350; (*b*) B. C. O'Regan, K. Bakker, J. Kroeze, H. Smit, P. Sommeling and J. R. Durrant, *J. Phys. Chem. B*, 2006, **110**, 17155–17160.

10 (*a*) F. Fabregat-Santiago, J. Bisquert, G. Garcia-Belmonte, G. Boschloo and A. Hagfeldt, *Sol. Energy Mater. Sol. Cells*, 2005, **87**, 117–131; (*b*) F. Fabregat-Santiago, G. Garcia-Belmonte, I. Mora-Sero and J. Bisquert, *Phys. Chem. Chem. Phys.*, 2011, **13**, 9083–9118.

11 (*a*) N. Cai, S.-J. Moon, C.-H. Le, T. Moehl, R. Humphry-Baker, P. Wang, S. M. Zakeeruddin and M. Grätzel, *Nano Lett.*, 2011, **11**, 1452; (*b*) S. H. Kim, H. W. Kim, C. Sakong, J. Namgoong, S. W. Park, M. J. Ko, C. H. Lee, W. I. Lee and J. P. Kim, *Org. Lett.*, 2011, **13**, 5784; (*c*) W.-F. Zhang, G.-M. Ng, H.-L. Tam, M.-S. Wong and F.-R. Zhu, *J. Polym. Sci., Part A: Polym. Chem.*, 2011, **49**, 1865.

12 (*a*) N. Kopidakis, K. D. Benkstein, J. van de Lagemaat and A. J. Frank, *J. Phys. Chem. B*, 2003, **107**, 11307–1131; (*b*) P. R. F. Barnes, A. Y. Anderson, J. R. Durrant and B. C. O'Regan, *Phys. Chem. Chem. Phys.*, 2011, **13**(13), 5798–5816.

13 (*a*) M. Wang, P. Chen, R. Humphry-Baker, S. M. Zakeeruddin and M. Grätzel, *ChemPhysChem*, 2009, **10**, 290–299; (*b*) M. Wang, X. Li, H. Lin, P. Pechy, S. Zakeeruddin and M. Grätzel, *Dalton Trans.*, 2009, 10015–10020.